JOURNAL OF APPLIED ELECTROCHEMISTRY 11 (1981) 493–502

The electrolytic oxidation of chromic sulphate to chromic acid: the effects of lead anode preparation

D. PLETCHER, S. J. D. TAIT

Department of Chemistry, The University, Southampton, UK

Received 23 September 1980

The electrolytic oxidation of chromic sulphate to chromic acid in a sulphuric acid medium has been examined at a number of lead dioxide surfaces (produced by the oxidation of lead containing 5% antimony either potentiostatically or by repetitive potential cycling), and has been characterized by cyclic voltammetry and other methods. The rate of the process and the current efficiency depend on the surface preparation to some extent.

1. Introduction

The anodic oxidation of chromic sulphate to dichromate in sulphuric acid solutions is an important industrial reaction. It is used to recycle solutions from the chromic acid oxidation of organic compounds, e.g. anthracene and montan wax, and to regenerate chromium electroplating solutions and chromic acid baths for electropolishing. A recent review [1] has confirmed that despite the wide application of the process [2], the literature concerning it is sparse and often contradictory. Certainly it is difficult to find details as to the optimum electrolysis conditions and although it is clear that lead dioxide is the only practical anode material, the effect of other electrolysis parameters is uncertain.

A major cause of the apparently irreproducible data is likely to be the lead dioxide anodes employed. The behaviour of lead dioxide must be expected to depend strongly on the method used for its preparation and its more recent history. Not only will the activity for chromium(III) oxidation be affected but also the rate of oxygen evolution, which always occurs simultaneously and reduces the current efficiency for chromic acid formation. Thus, for example, Kuhn and Birkett [3] have reported the disastrous effect of some organic compounds in the anolyte which result in the formation of an organic film on the electrode and high partial currents for oxygen evolution.

In this paper the anodic oxidation of lead, containing 5% antimony to improve its mechanical properties (note Hampson *et al.* [4–6] have compared the oxidation of Pb and Pb/Sb), to lead dioxide is carried out in several ways and cyclic voltammetry and other methods are used to examine the resulting surfaces. The oxidation of chromium(III) is then investigated on the various surfaces with the expectation that preparation of the lead dioxide will affect the current density and current efficiency for chromic acid formation and perhaps also the resistance of the anode to corrosion.

2. Experimental

The cyclic voltammetry was carried out using a Hi-Tek potentiostat, DT2101, and pulse generator, PPRI, and *I–E* responses were recorded on an *x–y* recorder (Hewlett Packard 7015A or Farnell DW 143B). Preparative electrolyses, steady-state *I–E* measurements and surface preparations requiring a high current were carried out using Chemical Electronics potentiostats, type 70 V/2 A or 25 V/20 A. Charges were measured using a laboratory-built integrator. An electron microscopy study was made using a Cambridge S-2A Stereoscan instrument.

All experiments were carried out in three-electrode glass cells. *I–E* data were recorded in a cell where the working electrode was a small lead/antimony (5%) disc surrounded by a PTFE sheath; this electrode entered the cell horizontally through

0021–891X/81/040493–10$03.00/0

a syringe barrel. A Pt counter electrode was in the same compartment and the SCE reference electrode was separated from the working electrode by a Luggin capillary and tap. The preparative electrolyses were carried out in a 'pipe' cell where the Pb/Sb working electrode and Pt counter electrode were parallel, separated by a glass sinter and entered the cell from opposite ends of a glass tube; the anolyte compartment was 10 cm^3. The working electrode (area $\simeq 2\ cm^2$) was surrounded by a PTFE sheath which had flanges machined on to it so that it sealed against a glass flange. The Luggin capillary entered the cell from the side and the whole cell was surrounded by a water jacket. Both cells had facilities for degassing the solutions with oxygen-free nitrogen. The reference electrode was always a Radiometer, type K410 SCE. Before each experiment the Pb/Sb working electrodes were rubbed with P.200 abrasive paper until a rough but shiny metallic finish was achieved and then washed with triply distilled water and 3 M H_2SO_4.

All solutions were prepared with triply distilled water, BDH Limited Analar sulphuric acid and reagent-grade chromic sulphate. Chromic acid concentrations were estimated by titration with ferrous ammonium sulphate with ferroin as an indicator.

3. Results and discussion

3.1. *The effect of preparation on a lead dioxide electrode*

The anodic oxidation of lead to lead sulphate and lead dioxide

$$\begin{aligned} Pb + SO_4^{2-} - 2e &\rightarrow PbSO_4 \\ PbSO_4 + 2H_2O - 2e &\rightarrow PbO_2 + 4H^+ + SO_4^{2-} \end{aligned} \qquad (1)$$

has been the subject of many papers because of the involvement of these reactions in the lead–acid battery (for bibliography see [7–9]). The positive electrode in a battery, however, has a porous paste structure quite unlike an electrode for use in an electrolytic process and in any case the oxidation of Cr(III) to Cr(VI) requires a potential more positive than generally necessary to recharge a battery positive electrode. Thus only a few papers [10–12] report cyclic voltammograms relevant to the present study.

The anodes for chromium oxidation were prepared by

(a) applying a constant potential in the Cr(III) solution for a fixed period;

(b) pre-electrolysis in 3 M H_2SO_4; again a controlled potential was applied for a fixed period;

(c) repetitive cycling of the potential through the range where PbO_2 is formed and reduced.

Thus in the first part of this paper we discuss the effect of potential limits on the layers formed during potential cycling. In the first series of experiments, a lead electrode was placed in 3 M H_2SO_4 at 0.0 V and the anodic current was allowed to fall to a very low value; the electrode was then subjected to a repetitive potential cycle between 0.0 V and a potential between + 2.0 V and + 2.3 V (see Figs. 1 and 2). In all cases during the initial scan from 0.0 V the *I–E* response shows an anodic peak at about + 0.2 V and some current is observed at all potentials, but on subsequent cycles the current below + 2.0 V quickly dies to a negligible value: the oxidation currents on the early cycles are due to thickening of the $PbSO_4$ layer formed at 0.0 V. Fig. 1a shows that when the scan is between 0.0 V and + 2.0 V at 0.3 V s^{-1}, the 25th cycle shows no distinct electrode processes. On increasing the positive limit to + 2.2 V or beyond, the *I–E* response on the 25th cycle shows three electrode processes, labelled A, B and C. As shown by the example of Fig. 2, the charge associated with processes A and C increases with cycling and, indeed, during the early cycles the peaks for processes A and C are barely visible (particularly when the limit is + 2.1 V). The peak for process C has the shape for the reduction of a surface layer and from the charge associated with the process, 280 mC cm^{-2} on the 80th cycle at 0–2.3 V, it is clearly a rather thick layer which is reduced. In common with earlier workers [10, 11, 13] we assign this peak to the overall reaction

$$PbO_2 + 4H^+ + SO_4^{2-} + 2e \rightarrow PbSO_4 + 2H_2O. \qquad (2)$$

By visual observation of the electrode, it is clear that process B is largely oxygen evolution. Process A must therefore be the formation of lead dioxide from lead sulphate (Reaction 1) and the absence of the peak in early cycles reflects the difficulty in forming nuclei of the PbO_2 phase in the highly resistive $PbSO_4$ layer. On the other hand, the nuclei, once formed, are not completely reduced

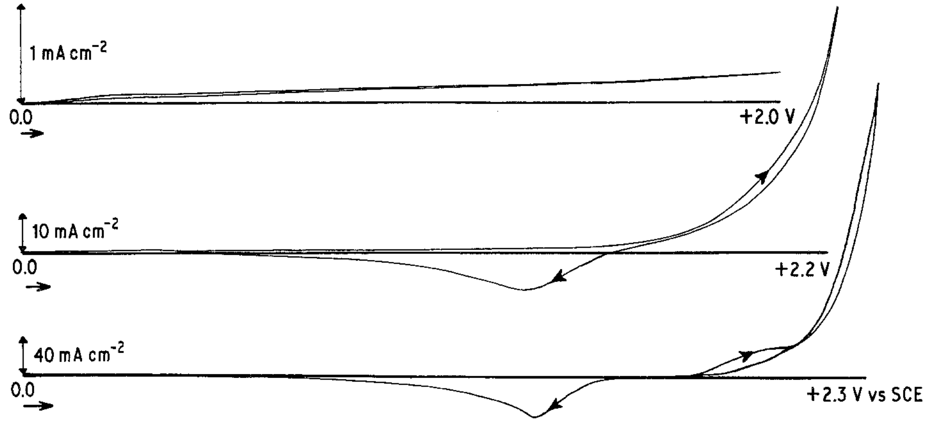

Fig. 1. 25th consecutive cyclic voltammogram of an antimonial lead electrode in 3 M H_2SO_4. Cycles between (a) 0.0 and + 2.0 V, (b) 0.0 and + 2.2 V, (c) 0.0 and + 2.3 V at 0.3 V s^{-1}.

during the scan towards negative potentials and hence they can start to grow again at lower overpotentials on following cycles. Thus process A is the oxidation of $PbSO_4$ to PbO_2 at already existing nuclei of PbO_2, while new nuclei of the oxidized phase are only formed at more positive potentials, at least at this potential scan rate.

Table 1 reports the results of an experiment where cyclic voltammograms are recorded between 0.0 V and a variable positive limit after an electrode has been formed by 100 potential cycles between 0.0 and + 2.3 V. The charge for process C indicates that the oxidation of $PbSO_4$ to PbO_2 is complete by + 2.1 V with this electrode (many PbO_2 nuclei exist in the surface layer after 100 cycles between 0.0 V and + 2.3 V). The current thereafter is totally oxygen evolution and the charge of 350 ± 20 mC cm^{-2} represents the total $PbSO_4$ accessible to oxidation while below + 1.8 V no significant PbO_2 formation occurs. This key

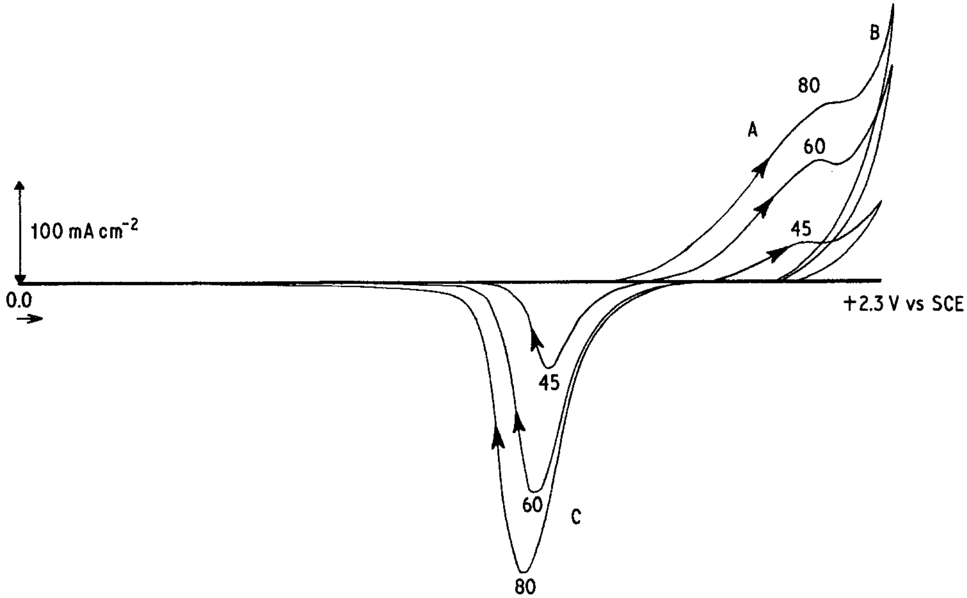

Fig. 2. 45th, 60th and 80th cyclic voltammograms of an antimonial lead electrode in 3 M H_2SO_4 between 0 and + 2.3 V at 0.3 V s^{-1} showing the progressive increase of peaks A and C.

Table 1. The variation in magnitude of peaks A and C as the positive potential limit is reduced by 100 mV per cycle during continuous cyclic voltammetry of an antimonial lead anode in 3 M H_2SO_4 at 0.3 Vs^{-1} after an initial 100 cycles between 0.0 and + 2.3 V versus SCE

Positive potential limit (V versus SCE)	*Process A*	*Process C*	
	Peak current density ($mA\,cm^{-2}$)	*Charge* ($mC\,cm^{-2}$)	*Peak potential* (V versus SCE)
+ 2.3	228	360	1.30
+ 2.2	224	337	1.30
+ 2.1	226	350	1.30
+ 2.0	200	241	1.34
+ 1.9	46	37	1.41
+ 1.8	0	0	–

potential depends, however, on potential scan rate and the nature of the experiment because of the time dependence of the nucleation process.

The cyclic voltammetric response for the lead dioxide electrode is markedly different if the pretreatment employs a cycle where the negative limit is + 1.0 V. Fig. 3 shows the *I–E* response during the 25th cycle between + 1.0 and 2.3 V at 0.3 $V\,s^{-1}$. Three differences between this curve and that in Fig. 1a should be noted: (a) the anodic currents on the scan to positive potentials are larger at all potentials, (b) a new anodic peak is observed at + 1.55 V (peak D), (c) at potentials negative to peak C, the cathodic current falls only to a limiting value (not zero). Peak D is more prominent if the potential scan is restricted to + 1.0 to + 1.8 V (following 80 cycles between + 1.0 V and + 2.3 V), as can be seen in Fig. 4. Moreover, with this scan, peak C changes shape towards that expected for a diffusion-controlled process and the peak currents for processes C and D are both proportional to the square root of potential scan rate; a similar cyclic voltammogram results from repetitive cycling of a fresh electrode between + 1.0 V and + 2.0 V.

Two further experiments were carried out to investigate the nature of peak D. Electrodes were prepared by cycling between + 1.0 V and + 2.3 V (see Fig. 3). Then in the first experiment the electrode potential was cycled once between + 1.0 V and + 2.3 V, held at 1.0 V for 10 s or 100 s and then the *I–E* response between + 1.0 V and

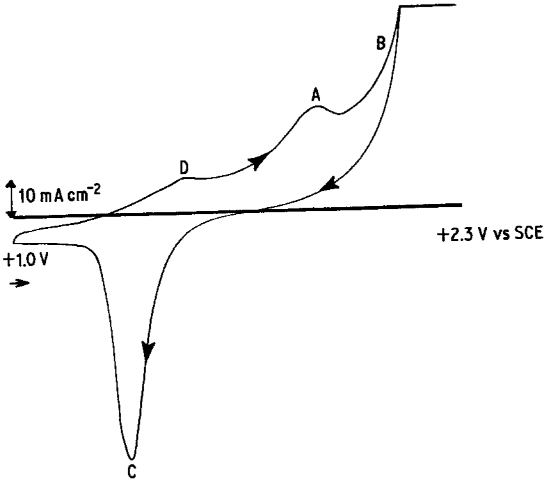

Fig. 3. 25th consecutive cyclic voltammogram of a Pb/Sb electrode in 3 M H_2SO_4 run between + 1.0 and + 2.3 V at 0.3 $V\,s^{-1}$.

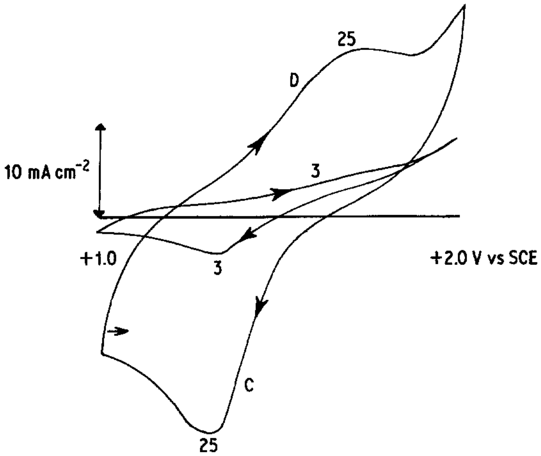

Fig. 4. 3rd and 25th cyclic voltammograms of a Pb/Sb electrode in 3 M H_2SO_4 run between + 1.0 and + 2.0 V at 0.3 $V\,s^{-1}$.

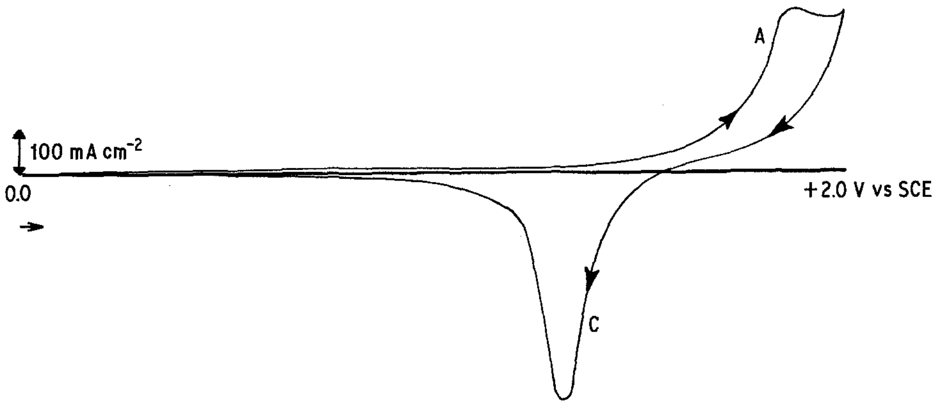

Fig. 5. First potential cycle of a Pb/Sb electrode in 3 M H_2SO_4 run between 0 and + 2.0 V at 0.3 V s^{-1} after discharge at + 2.0 V for 20 min in 3 M H_2SO_4.

+ 2.3 V was recorded; in both cases, peak D was absent, though when the period at 1.0 V was 10 s, a peak was seen at a more positive potential (+ 1.78 V). In the second experiment the electrode potential was cycled once between + 1.0 V and + 2.3 V, then pulsed to 0.0 V for 0.4 s before being swept between + 1.0 and + 2.3 V: peak D was again absent.

These observations can be explained if it is recognized that nuclei of PbO_2 are more likely to survive without reduction if the potential scan is limited to + 1.0 V and that the reduction of PbO_2 to $PbSO_4$ is a complex multistep process. Thus we would postulate that process D is the reoxidation of an intermediate in this reduction, for example

$$PbO_2 + 2H^+ + 2e \rightarrow PbO + H_2O$$

$$PbO + H_2SO_4 \xrightarrow{\text{slow}} PbSO_4 + H_2O \qquad (3)$$

$$PbO + H_2O - 2e \longrightarrow PbO_2 + 2H^+ \qquad (4)$$

in which case peak D (Reaction 4) will only be observed if there is insufficient time for the sulphation of PbO to occur completely (the potential excursion to 0.0 V is also a time lag) and some nuclei of PbO_2 remain (this will depend on both potential and time). Moreover, the peaks in Fig. 4 would then be for the couple PbO/PbO_2 and presumably the current is diffusion controlled with respect to a species, e.g., proton, in the solid state.

It is, however, also possible that the cyclic voltammetric response is determined by changes in morphology caused by cycling the potential to very positive values. Indeed with the $PbSO_4/PbO_2$ electrode it is difficult to deduce a unique explanation because of the complexity of the system which arises, principally from five factors. These are: (a) the oxidized and reduced forms are, in fact, mixtures of Pb(IV) and Pb(II) species respectively, (b) both the oxidized and reduced forms are crystalline solids and interchange involves nucleation and growth, each with its own time and potential dependences, (c) the interconversion of $PbSO_4$ and PbO_2 is a multistep process, at least two electron transfers, two proton transfers and a

Table 2. Effect of pretreatment on the oxidation and reduction of Pb/Sb (medium: 3 M H_2SO_4)

Pretreatment	*Process A*		*Process C*	
	E_p (V versus SCE)	I_p (mA cm^{-2})	E_p (V versus SCE)	Q_p (mC cm^{-2})
+ 2.0 V for 20 min	1.87	350	1.31	642
80 cycles 0.0–2.3 V at 0.3 V s^{-1}	2.00	225	1.27	304
80 cycles 1.0–2.3 V at 0.3 V s^{-1}	1.92	280	1.34	594

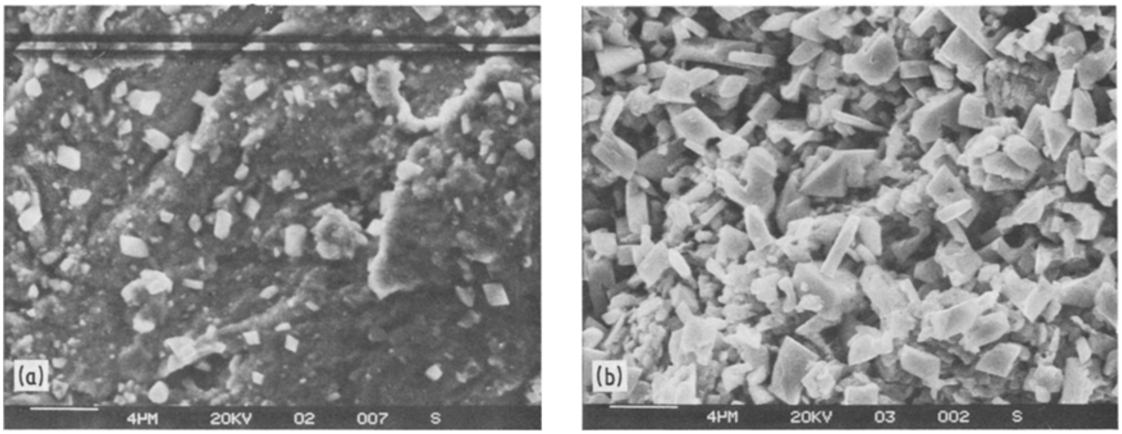

Fig. 6. Electron micrographs of $PbSO_4$ surface resulting from (a) 100 cycles and (b) 1000 cycles of potential between 0.0 and + 2.0 V. Pb/Sb electrode in 3 M H_2SO_4, scan rate 0.3 V s^{-1}.

sulphation/desulphation step, (d) the poor conductivity of $PbSO_4$, (e) the properties of the porous layer, which make the process subject to pore blocking and affect the availability of reactants, e.g. the pH in the pores may differ totally from the bulk solution. It was not, however, the purpose of this work to seek detailed explanations of the $PbO_2/PbSO_4$ couple but only to confirm the possibility of forming different anodes.

Further PbO_2 anodes were prepared potentiostatically and Fig. 5 shows the cyclic voltammogram for an electrode prepared at + 2.0 V for 20 min. The only processes visible are A and C. The characteristics of processes A and C for the electrodes resulting from the various preparations are summarized in Table 2. Clear differences in the amount of oxidation and reduction can be seen although it is not clear to what extent this reflects differences in surface area, thickness of the oxidized layer or accessibility of reactants in the porous layer. The difference in the surfaces with method of preparation is, however, fully confirmed by electron microscopy. For example, Fig. 6 compares the lead sulphate surfaces resulting from 100 and 1000 cycles between 0.0 and + 2.0 V (the crystallinity of the surfaces clearly increases with cycle number) while Fig. 7 compares the surfaces resulting from different surface preparations.

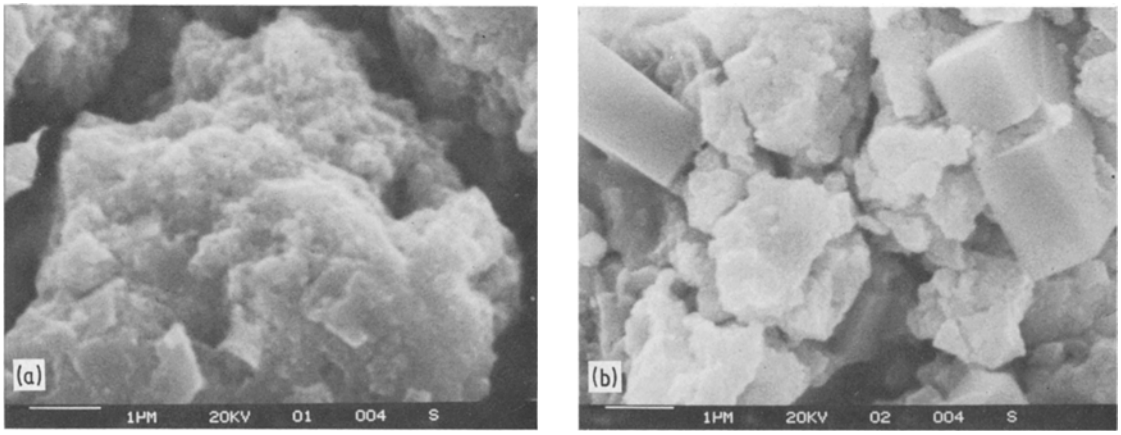

Fig. 7. Electron micrographs of PbO_2 surface resulting from (a) 100 cycles between 0.0 and + 2.3 V at 0.3 V s^{-1} and (b) 20 min at + 2.0 V. Pb/Sb electrode in 3 M H_2SO_4.

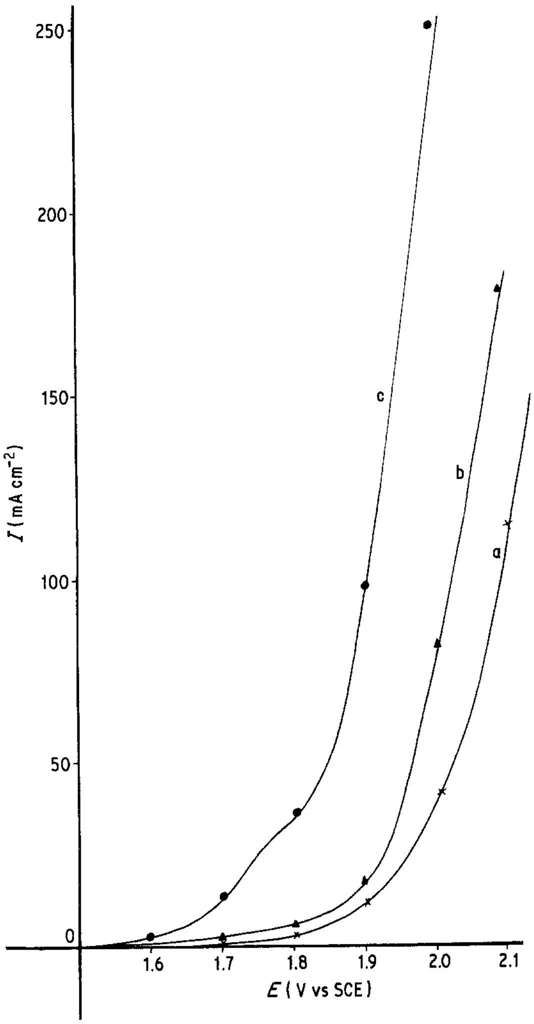

Fig. 8. Variation of current density with potential for a Pb/Sb electrode (pretreated by 10 cycles at 30 mV s^{-1} between + 1.0 and + 2.0 V in 3 M H_2SO_4) in (a) 3 M H_2SO_4, (b) 0.2 M Cr(III)/3M H_2SO_4, (c) 2.0 M Cr(III)/ 3 M H_2SO_4.

3.2. *The oxidation of chromium(III) to chromic acid*

Cyclic voltammograms for 3 M H_2SO_4 + 0.2 M Cr(III) run at electrodes prepared in sulphuric acid were not significantly different from those for the acid alone although there was some increase in current at potentials positive to peak A. Hence the experimental approach was to combine the measurement of steady-state *I–E* curves with measurement of current efficiencies from preparative electrolyses.

The first experiments sought to define the effect of electrolysis parameters using lead dioxide anodes prepared by 10–15 cycles between + 1.0 V and + 2.0 V at 30 mV s^{-1}. Fig. 8 shows *I–E* curves for 3 M H_2SO_4 and two concentrations (0.2 M and 2.0 M) of Cr(III) in the acid. It can be seen that the current increases with chromium concentration at all potentials above + 1.6 V and as expected the current increases with potential. At no potential did the current approach the value expected for mass-transfer control and it was unaffected by agitation of the solution. With solutions of Cr(III) above 1 M, the data were not entirely reproducible when the temperature was below 40° C. This problem was associated with a yellow deposit [3, 14] which was formed on the anode in some experiments; when the deposit was present, the current increased with time at each potential. Table 3 reports the current efficiency (at three conversions) for the formation of chromic acid from 0.2 M Cr(III) and also the initial current density as a function of potential; the highest current efficiency is observed at + 1.75–1.80 V but at these potentials

Table 3. Current density and current efficiency for the oxidation of Cr(III) to Cr(VI) in 3 M H_2SO_4 + 0.2 M Cr(III). Electrodes pretreated with 15 cycles from +1.0 V–2.0 V at 30 mV s^{-1} in 3 M H_2SO_4

Potential (V versus SCE)	*Current density* (mA cm^{-2})	*Current efficiency (%) after charges* (F mol^{-1} Cr(III))		
		0.15	*0.75*	*1.5*
1.75	2.9	86	83	86
1.80	9.6	88	83	88
1.90	21.1	68	66	62
2.00	77	–	65	38

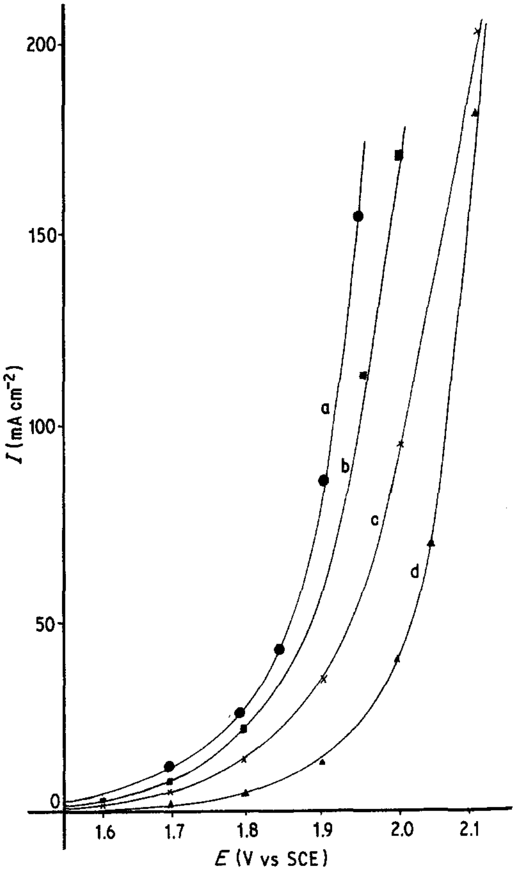

Fig. 9. Variation of current density with potential for 1 M Cr(III)/3 M H_2SO_4 at a Pb/Sb electrode pretreated by 10 cycles at 30 mV s^{-1} in 3 M H_2SO_4, between the potential limits of + 1.0 V and (a) + 2.0 V, (b) + 2.1 V, (c) + 2.3 V. Curve (d) shows the variation in 3 M H_2SO_4 alone.

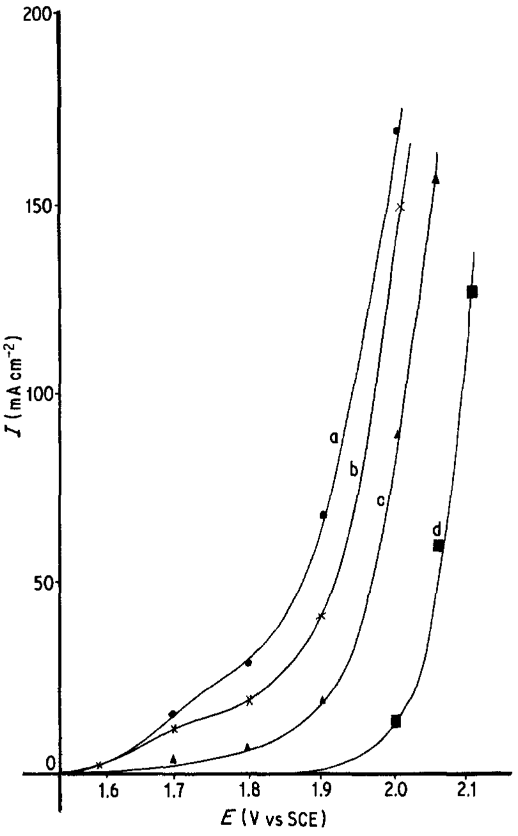

Fig. 10. Variation of current density with potential for 1.0 M Cr(III)/3 M H_2SO_4 at a Pb/Sb electrode pretreated by 100 cycles between + 1.0 V and + 2.0 V at sweep rates of (a) 30 mV s^{-1}, (b) 300 mV s^{-1}, (c) 3 V s^{-1}. The corresponding curve without pretreatment is shown as (d).

the current density is relatively poor. Increasing the Cr(III) concentration certainly increased the current density and also improved the current efficiency to some extent; for example, at + 1.9 V the current efficiency was 68%, 82% and 62% for 0.2 M, 1.0 M and 2.0 M Cr(III) respectively. The drop at the highest concentration could again be attributed to the formation of the yellow deposit on the anode. An increase in temperature also increased the current density but had little effect on current efficiency at 1.9 V and using 1.0 M Cr(III) (82%, 78% and 79% at 35, 50 and 65° C respectively). The major advantage of increasing the temperature was that the unwanted yellow deposit was never obtained and currents were therefore more reproducible.

Table 4. Current efficiency for the oxidation of 1 M Cr(III) in 3 M H_2SO_4 as a function of electrode preparation ($E = 1.9$ V versus SCE)

Electrode preparation	*Current efficiency after 0.15 F mol^{-1}*
Cycle 1.0–2.1 V at 0.3 V s^{-1} for 15 min	82
2.0 V for 20 min	112
None	92

The method of preparation of the lead anode had a marked effect on steady-state *I–E* curves for the oxidation of Cr(III) and two examples are given in Figs. 9 and 10 where it can be seen that the preparation can increase the current by an order of magnitude. Table 4 also shows that early in the electrolysis the current efficiency also varies

Table 5. Variation in current efficiency and current density after 0.11 F mol^{-1} for the oxidation of Cr(III) to Cr(VI) in 3 M H_2SO_4. Electrodes not pretreated; electrode potential +1.9 V versus SCE

Cr(III) concentration (M)	*Temperature* (° C)	*Current efficiency* (%)	*Final current density* (mA cm^{-2})
1	25	92	78
1	45	86	248
1	65	93	497
3	25	100	99
3	46	101	320
3	70	104	570

with preparation. The long-term effects of surface pretreatment are less certain because, on a long timescale, current densities tended to a similar value. Moreover, it can be seen in Table 4 that current efficiency could exceed 100% and this must be explained by chemical oxidation of Cr(III) by PbO_2 formed during pretreatment; such a reaction will clearly produce a massive change in the PbO_2 surface.

Table 5 reports data for preparative electrolyses using lead electrodes which were not pretreated in any way. In contrast to the pretreated anodes which reached a steady-state current rapidly, the current in these experiments increased continuously with time (e.g. at 40° C the current change was from 30 to 320 mA cm^{-2}) and the final current at a 5% conversion was about 10% higher than that with an electrode prepared by cycling between +1.0 and +2.0 V for 15 min. The interesting features of the data in Table 5 are the high current efficiencies at a current density exceeding that used in industrial practice (100–200 mA cm^{-2}) and similar performance was obtained immediately with pretreated anodes. While it appears for the data in Table 5 that the current density is not very dependent on the chromium(III) concentration, it should be remembered that these currents had not reached a steady-state value.

Because of our interest in coupling the electrolytic generation of the dichromate to its reactions in organic solvents using phase transfer catalysis [15], a series of experiments was carried out to test the effect of the components of the system on the efficiency of chromium(III) oxidation. The results are reported in Table 6. It may be seen that methylene chloride and tetrabutylammonium ions do not adversely effect the current efficiency but partially water-soluble organic compounds such as benzyl alcohol and octanol cause a substantial fall in the current efficiency although some recovery occurs on continued electrolysis, presumably because all the organic compound is consumed. These observations agree entirely with those of Birkett and Kuhn [3].

Table 6. The effect of organic contaminants on the regeneration of Cr(VI). All experiments were completed at 60° C in 0.5 M Cr(III)/3 M H_2SO_4 at + 1.9 V versus SCE on Pb/Sb surfaces pretreated with 15 min discharging at + 2.0 V in 3 M H_2SO_4

Pretreatment of the 0.5 M Cr(III)/3 M H_2SO_4 solution	*Current efficiency (%) after:*		*Final current density* (mA cm^{-2})
	0.3 F mol^{-1}	*1.38 F mol^{-1}*	
1. None	101	–	350
2. After shaking with $N(Bu)_4^+HSO_4^-$ in $(CH_2Cl)_2$	103	–	210
3. By reaction of 0.25 M $Cr_2O_7^{2-}$ with $C_6H_5CH_2OH$†	0	39	570
4. As 3 above, only with octanol	39	57	550
5. As 4 above with no $N(Bu)_4^+HSO_4^-$	–	58	–

† The 0.5 M Cr(III) solution was prepared by shaking 0.25 M $Cr_2O_7^{2-}$/3 M H_2SO_4 with the slight excess of $C_6H_5CH_2OH$ in the presence of $N(Bu)_4^+HSO_4^-$.

4. Conclusions

The use of high chromium(III) concentrations and elevated temperature is highly advantageous. The oxidation of chromium(III) to chromic acid is possible almost quantitatively at low conversions (the conditions generally used when the cell is coupled directly to an organic oxidation), and the current density can be in excess of 0.5 A cm^{-2} when the temperature is 70° C and the chromium(III) concentration above 1 M. The experimental data are, however, also very dependent on the pretreatment of the surface and/or history of the anode and these factors probably account for the contradictory information in the literature [1] concerning the effect of electrolysis parameters, e.g., temperature, concentration of Cr(III). The data, although obtained under conditions of controlled potential, would also indicate that it should be possible to run industrial cells at higher current densities (>0.5 A cm^{-2}). It would be necessary to define a suitable starting-up procedure, for example where the current density was programmed to increase slowly.

References

[1] A. T. Kuhn and R. Clarke, *J. Appl. Chem. Biotechnol.* **26** (1976) 407.
[2] G. L. Mantell, 'Electrochemical Engineering', McGraw-Hill, New York (1960).
[3] A. T. Kuhn and M. Birkett, *J. Appl. Electrochem.* 9 (1979) 777.
[4] N. A. Hampson, S. Kelly and K. Peters, *ibid* **10** (1980) 91.
[5] *Idem, ibid* **10** (1980) 261.
[6] N. A. Hampson, S. Kelly, K. Peters and P. Whyatt, *ibid* **10** (1980) 597.
[7] J. P. Carr and H. A. Hampson, *Chem. Rev.* **72** (1972) 679.
[8] G. Kelsall, Electricity Council Research Centre Report N1060 (1977).
[9] H. Bode, 'Lead-Acid Batteries', John Wiley and Sons, New York (1977).
[10] T. G. Chang, M. M. Wright and E. M. L. Valeriote, *Power Sources* **6** (1977) 69.
[11] P. Casson, N. A. Hampson and K. Peters, *J. Electrochem. Soc.* **124** (1977) 1655.
[12] *Idem, J. Electroanal. Chem.* **83** (1977) 87.
[13] S. G. Canagaratna, P. Casson, N. A. Hampson and K. Peters, *ibid* 79 (1977) 273.
[14] J. Mizuguchi, *J. Electrochem. Soc. Japan* 19 (1951) 16.
[15] D. Pletcher and S. J. D. Tait, *J. Chem. Soc., Perk II* (1979) 788.